the plant journal

SEB SOCIETY FOR EXPERIMENTAL BIOLOGY

The Plant Journal (2020) **101,** 1287–1302 doi: 10.1111/tpj.14590

CONSTANS–FKBP12 interaction contributes to modulation of photoperiodic flowering in Arabidopsis

Gloria Serrano-Bueno[1,†], Fatima E. Said[1,†], Pedro de los Reyes[1], Eva I. Lucas-Reina[1,‡], M. Isabel Ortiz-Marchena[1], José M. Romero[1,2] and Federico Valverde[1,*]

[1]*Instituto de Bioquímica Vegetal y Fotosíntesis, CSIC-Universidad de Sevilla, 49 Americo Vespucio, 41092 Sevilla, Spain ,*
[2]*Departamento de Bioquímica Vegetal y Biología Molecular, Facultad de Biología, Universidad de Sevilla, Reina Mercedes, 41012 Sevilla, Spain*

Received 24 June 2019; accepted 21 October 2019; published online 29 October 2019.
*For correspondence (e-mail federico.valverde@ibvf.csic.es).
†These authors contributed equally to this work.
‡Present address: Departamento de Biología Molecular y Bioquímica, Facultad de Ciencias-Universidad de Málaga, Instituto de Hortofruticultura Subtropical y Mediterránea-Universidad de Málaga-CSIC, 29071 Málaga, Spain

SUMMARY

Flowering time is a key process in plant development. Photoperiodic signals play a crucial role in the floral transition in *Arabidopsis thaliana*, and the protein CONSTANS (CO) has a central regulatory function that is tightly regulated at the transcriptional and post-translational levels. The stability of CO protein depends on a light-driven proteasome process that optimizes its accumulation in the evening to promote the production of the florigen FLOWERING LOCUS T (FT) and induce seasonal flowering. To further investigate the post-translational regulation of CO protein we have dissected its interactome network employing *in vivo* and *in vitro* assays and molecular genetics approaches. The immunophilin FKBP12 has been identified in Arabidopsis as a CO interactor that regulates its accumulation and activity. FKBP12 and CO interact through the CCT domain, affecting the stability and function of CO. *fkbp12* insertion mutants show a delay in flowering time, while *FKBP12* overexpression accelerates flowering, and these phenotypes can be directly related to a change in accumulation of FT protein. The interaction is conserved between the *Chlamydomonas* algal orthologs CrCO–CrFKBP12, revealing an ancient regulatory step in photoperiod regulation of plant development.

Keywords: CONSTANS, FKBP12, floral transition, photoperiodic flowering, post-translational modification, protein stability.

INTRODUCTION

The precise timing of the floral transition is a key decision for a plant, as it is directly related to the success of its offspring (Austen *et al.*, 2017). The floral transition is influenced by internal and external cues that determine the correct time of year to flower (Levin, 2009). The recent literature has unveiled an intricate network of genes involved in the floral transition in the model plant *Arabidopsis thaliana* (Pajoro *et al.*, 2014). The vernalization (Song *et al.*, 2012), photoperiodic and internal (Andrés and Coupland, 2012) pathways define well-delimited, but still interconnected, pathways that control the floral transition in Arabidopsis (Blümel *et al.*, 2015).

The photoperiod pathway involves the response of the plant to the length of the day and the way it will flower in response to changes in light-driven circadian rhythms (Shim *et al.*, 2017). Thus, *A. thaliana* is a facultative long-day (LD) plant that will flower earlier under a 16-h light/8-h dark day than under a short day (SD) of 8-h light/16-h dark. However, other plants, such as rice, will respond differently by flowering when daylight recedes, and some may not even respond to day length, as in the case for some wild tomato species (Jackson 2009). The gene *CONSTANS* (*CO*) plays a pivotal role, as CO protein binds in a complex to the promoter of the florigenic gene *FLOWERING LOCUS T* (*FT*) (Wenkel *et al.*, 2006; Tiwari *et al.*, 2010; Gnesutta *et al.*, 2017) inducing its expression under LD conditions in the phloem companion cells (An *et al.*, 2004). Then, FT protein will move through the phloem to the shoot apical meristem to induce the activation of the floral developmental program (Mathieu *et al.*, 2007).

CONSTANS will also activate the expression of several genes involved in the transmission of this flowering signal, such as the starch synthase *GBSS*, which promotes a

temporal increase in the concentration of soluble sugars during the floral transition (Ortiz-Marchena *et al.*, 2014) or proline synthesis (Mattioli *et al.*, 2009). Thus, the photoperiod pathway also controls signals, such as an increase in mobile sugars from starch (Ortiz-Marchena *et al.*, 2015), that would systemically coordinate this transition.

Most of the accumulated information on flowering time control involves changes at the transcriptional level (Guo *et al.*, 2017), but important post-translational steps are also pivotal to this process (Swiezewski *et al.*, 2009; Posé *et al.*, 2013). CONSTANS protein is particularly sensitive to post-translational modifications, with both phosphorylation (Sarid-Krebs *et al.*, 2015) and ubiquitination (Valverde *et al.*, 2004) playing important roles in its stability. In these signaling processes the RING finger E3 ubiquitin ligases CONSTITUTIVE PHOTOMORPHOGENIC 1 (COP1) and HIGH EXPRESSION OF OSMOTICALLY RESPONSIVE GENE 1 (HOS1) act in a stepwise manner to control the nocturnal (COP1) and early morning (HOS1) proteasome-mediated degradation of CO, limiting its presence to LD evenings (Jang *et al.*, 2008; Lazaro *et al.*, 2012). Also, blue light through cryptochrome 2 (CRY2), affecting COP1 (Valverde *et al.*, 2004), and red light through phytochrome B (PHYB), affecting HOS1 (Lazaro *et al.*, 2015), are important in this process.

The small immunophilin FKBP12 (FK506 binding protein 12 kDa) has been thoroughly characterized in animals as an immunorepressor, due to its capacity to bind and inhibit the phosphatase calcineurin through the drug K506 (tacrolimus) (Kang *et al.*, 2008). FKBP12 can also bind TOR (target of rapamycin) kinase by forming a covalent bond rapamycin–FKBP12-TOR that inactivates this essential kinase (Loewith *et al.*, 2002). Although algae such as *Chlamydomonas* are sensitive to rapamycin (Crespo *et al.*, 2005), higher plants are mostly insensitive to this drug because plant FKBP12 lacks the key amino acid residues that mediate the interaction with TOR (Menand *et al.*, 2002). This has been proposed to be an evolutionary acquisition of spermatophytes in response to their long cohabitation with rapamycin-producing bacteria in the soil (Xiong and Sheen, 2012). Arabidopsis FKBP12 has the prolyl isomerase activity that characterizes all FKBP family members, which are able to alter the state of proline residues within a polypeptide chain from *cis* to *trans* forms (Gollan *et al.*, 2012), thus having a crucial role in protein structure. The FKBPs have also been involved in supramolecular complexes that help partners modify their structure, identify substrates and move through cellular compartments (Kim and Chen, 2002). Although some *fkbps* mutants display a strong developmental phenotype, plant *fkbp12* mutants have not been described in detail and no phenotypic description of its mutation or developmental defects has been given. In fact, only a single partner of FKBP12, namely FKBP12 INTERACTING PROTEIN 37 (AtFIP37) (Faure *et al.*, 1998) has been identified in plants, and a role in trichome endoreduplication proposed (Vespa *et al.*, 2004).

In this work, we describe an alternative role for FKBP12 in the post-translational modification of CO in Arabidopsis. The interaction with FKBP12 influences the stability of CO and promotes its activity. Therefore, CO activity is compromised not only by the action of photoreceptors, ubiquitin ligases and protein kinases but also through the interaction with the small chaperone-like FKBP12. The CO–FKBP12 interaction involves the same domain that mediates COP1 and HOS1 interaction, and therefore could also interfere with the stability of CO. Both mutant and overexpression lines show a slight but consistent floral phenotype that can be traced to small changes in *FT*, but not *CO*, expression patterns. The interaction is conserved between the *Chlamydomonas reinhardtii* homologous proteins CrCO (Serrano *et al.*, 2009) and CrFKBP12 (Crespo *et al.*, 2005), providing a clue to the evolutionary importance of the complex. Therefore, this work unveils a different role for modification of CO activity at the post-translational level that could be important for understanding and modifying flowering time in other plant species such as crops.

RESULTS

Identification of FKBP12 as a CONSTANS-interacting protein

In order to identify other binding partners involved in post-translational regulation of CONSTANS, the yeast-based split-ubiquitin system (SUS) approach was used (Johnsson and Varshavsky 1994; Pusch *et al.*, 2012). As CO can self-activate transcription in traditional yeast two-hybrid (Y2H) screenings (Ben-Naim *et al.*, 2006), an assay exclusively based on protein interactions was chosen. A library constructed from 4-week-old plants grown in LD conditions and harvested during daylight (I. Ottenschläger and F. Santos, K. Palme Laboratory) was screened. In this SUS version, the prey vector includes Arabidopsis cDNA library clones fused to the N-terminal part of ubiquitin attached to the *URA3* gene. *URA3* codes for the enzyme R-URA, which catalyzes the synthesis of the toxin 5-fluorouracil from the protoxin 5-FOA (5-fluoroorotic acid). In the bait vector, the CO open reading frame (ORF) is fused to ubiquitin C-terminal part. Reconstitution of ubiquitin, meaning interaction between prey and bait, degrades the R-URA protein (by the proteasome), allowing the growth of colonies in the presence of 5-FOA and the selection of clones expressing the interacting proteins (Dünnwald *et al.*, 1999). This allowed us to use the whole CO protein rather than isolated domains (Wenkel *et al.*, 2006) or artificial fusions (Ben-Naim *et al.*, 2006) and opened up the possibility of describing different interactions.

We conducted five independent SUS experiments: more than 25 000 independent interactions were tested and 42

Table 1 Interactors with CONSTANS protein in the split ubiquitin system

Gene identifier	Protein name	Protein description
At3g52360	–	Endomembrane protein involved in karrikin response
At2g20420	ATP citrate lyase (ACL)	Succinate-CoA ligase (GDP-forming) activity
At1g02290	NFRKB-RELATED	Related to kappa-B binding protein, IN080 complex
At2g40430	SMO4	Regulator of cell division in organ growth
At2g44065	Ribosomal protein	Structural constituent of ribosome
At3g27350	–	Nuclear protein of unknown function
At5g05370	Cytochrome b-c1 complex, subunit 8	Respiratory chain component
At4g31985	RPL39C	Structural constituent of ribosome
At2g421190	–	rho GTPase-activating gacO-like protein
At4g29390	RPS30D	Structural constituent of ribosome
At1g71695	PPXR6	Peroxidase protein; response to oxidative stress
At3g52500	Aspartyl protease	Aspartic-type endopeptidase activity
At5g17960	C1-clan protein	Hormone stress response
At3g211160	MNS2	*N*-glycan processing, root development
At1g58080	HISN1A	ATP phosphoribosyltransferase, histidine biosynthetic process
At3g60640	ATG8G	Autophagy, cellular response to nitrogen starvation, protein transport, nuclear
At3g09840	CDC48A	Cell division cycle protein, member of AAA-type ATPase family
At3g281180	CSLC4	Cellulose synthase, cell wall organization
At1g29930	LHCB1.3	LHCII complex subunit, photosynthesis, response to light stimuli
At5g64350	FKBP12	Chaperone-mediated protein folding, peptidyl-proline modification, protein peptidyl-prolyl isomerization
At2g471180	GOLS1	Galactinol synthase, formation of galactinol from UDP-galactose and myo-inositol, hexosyltransferase
At3g26650	GAPDHA1	Photosynthetic glyceraldehyde-3-phosphate dehydrogenase
At1g211130	IGMT4	Methyltransferase activity, protein dimerization activity
At3g57300	IN080	Member of the SWI/SNF ATPase family, chromatin remodeling
At2g38530	LTP2	Involved in lipid transfer between membranes,cell growth
At5g02380	MT2B	Metallothionein, cysteine-rich protein with copper-binding activity
At3g20970	ATNFU2	Contains NUF domain, iron-sulfur cluster assembly
At3g61990	OMTF3	Methyltransferase involved in the methylation of plant transmembrane proteins
At5g42790	PAF1	Extensive homology to the largest subunit of the multicatalytic proteinase complex (proteasome)
At3g25800	PP2A-A2	One of three protein phosphatase 2A regulatory subunits
At5g41700	UBC8	Constituent of the ubiquitin-conjugating enzyme E2

positive clones, representing 31 different putative CO-binding partners, were identified (Table 1). The putative CO interactors were grouped according to functional terms using the agriGO and TAIR tools (Figure S1a,b in the online Supporting Information). Gene Ontology terms that were significantly enriched among these interactors were related to macromolecular interactions (DNA/RNA and proteins), transferase/hydrolase activity and stress/biotic/abiotic stimulants. Fifteen of the proteins were predicted as nuclear, but others were allocated to organelles or the cytosol, reflecting the wide range of possible interactions allowed by the SUS protocol. Even considering that some of them might be artifactual, cytosolic interactors have previously been described as important regulators of transcription factors (TFs) (Cyert, 2001; Igarashi *et al.*, 2001; Wilson *et al.*, 2016).

Among these interactors, clones including the small immunophilin FKBP12 (At5g64350) (Table 1, highlighted in grey) were repeatedly rescued in the SUS screening. In fact, tomato FKBP12 had been previously identified as a putative interactor of a CO homolog (SlCOL1) in Y2H screening using a tomato cDNA library (Ben-Naim *et al.*, 2006). As FKBPs are mainly cytosolic proteins and several reports have shown that they could act as chaperones involved in protein folding and cellular transport (Geisler and Bailly, 2007; Gollan *et al.*, 2012), they were excellent candidates for CO post-translational regulators.

Interaction between CO and FKBP12

The interaction of CO and FKBP12 was confirmed by experiments in bacteria, yeast and plants. First, *CO* and *FKBP12* complete ORFs were expressed in *Escherichia coli* under the same inducible promoter (pETDuet-1, see Experimental Procedures) so that upon induction by isopropyl-β-thio-galactopyranoside (IPTG) both proteins were produced

with a similar stoichiometry (Figure S3a). To identify the polypeptides, CO was S-tagged (S·CO) and FKBP12 His-tagged (H·FK) (Figures 1a,b and S3a). When the extracts were incubated with TALON His-affinity resin and washed, immunoblots using αHis showed that H·FK was retained in the beads (Figure 1a, lanes Ft, W) and eluted by increasing imidazole concentration (Figure 1a, lane El). When the same blot was restriped and tested with a specific CO antibody (αCO, see Experimental Procedures) we found that S·CO was effectively co-expressed with H·FK (Figure 1a, lane In), but further, the interaction was confirmed by showing that S·CO was retained (Figure 1a, lanes Ft, W) and co-eluted in the same fraction as H·FK (Figure 1a, lane El). Controls in which S·CO alone were expressed in *E. coli* showed that CO had a very low affinity for TALON resin (Figure 1b).

A transient interaction assay in *Nicotiana benthamiana* cells was used to further test CO–FKBP12 interaction. The CO ORF was fused at the carboxyl end to yellow fluorescent protein (CO–YFP) and FKBP12 was fused to cyan fluorescent protein (FK–CFP). The fluorescent constructs were transiently expressed in *N. benthamiana* via *Agrobacterium tumefaciens* transformation (Voinnet *et al.*, 2003) and observed under a confocal microscope (Figures 1c and S2). While FK–CFP alone showed a mainly cytosolic localization in *N. benthamiana* cells (Figure S2a) and CO–YFP, as expected, was located in the nucleus (Figure S2b), surprisingly, co-expression of both constructs showed a nuclear–cytosolic signal in *N. benthamiana* in both yellow and blue light when excited at their corresponding exciting light wavelengths (Figure S2c). When the same plants were excited with specific CFP-exciting lights and detected at the YFP emission window, the nuclear–cytosolic signal (Figure 1c) indicated a fluorescence resonance energy transfer (FRET) effect. This effect was quantified with an efficiency 10–20% higher than that of the control including FK–CFP and the yellow protein alone (Figures 1c, right, and S2e). The FRET effect strongly supported direct *in vivo*

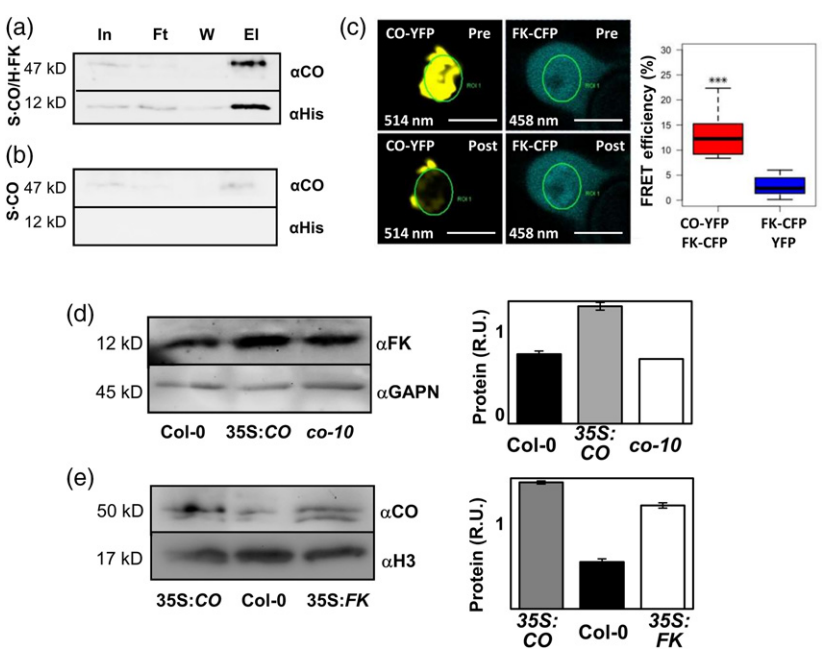

Figure 1. Interaction between CONSTANS (CO) and FKBP12.
(a) Co-elution of S-tagged CO (S·CO) with His-tagged FKBP12 (H·FK) in *Escherichia coli*. Immunoblots show the presence of S·CO (above) and H·FK (below) in soluble extract (Introduction, In), binding to S·beads (Flow through, Ft), washing with buffer (W) and elution (El). αCO (above) and αHis-tag (below) antibodies were used.
(b) Control experiment in which S·CO is expressed alone.
(c) Confocal images of *Nicotiana benthamiana* leaves co-infiltrated with 35S:FKBP2:CFP tag (FK-CFP, cyan) and 35S:CO:YFP (YFP-CO, yellow) constructs. Fluorescence resonance energy transfer (FRET) was measured by the acceptor photobleaching technique. The white bar represents 10 μm. The quantified efficiency of the interaction (blue) and negative control (red) is shown on the right.
(d) Immunoblots showing FKBP12 in total soluble fractions of Col-0, 35S:CO and *co-10* plants 15 days after germination (DAG) under long-day (LD; 16-h light/8-h dark) conditions (left). Seventy micrograms of protein was loaded per lane and probed with αFK (above) or antibody against cytosolic non-phosphorylating GAPDHN (αGAPN, below) as a loading control. The FKBP12 signal was quantified compared with the control in three independent experiments and plotted (right).
(e) Immunoblots showing CO levels in nuclear fractions of 35S:CO, Col-0 and 35S:FK plants (15 DAG, LD). One hundred micrograms of protein from nuclear lysates was probed with αCO (above) and αHistone3 (αH3, below). The CO signal was quantified compared with the control in three independent experiments and plotted (right).

interaction between both proteins. A co-expression experiment was repeated in onion epidermal cells by transient particle bombardment assays, showing a clear co-localization signal (Figure S2d). The interaction in *N. benthamiana* was also tested by co-immunoprecipitation experiments. In this experiment, we used the same CO–YFP plants and FK–TAP plants that fused FKBP12 to the TAP tag at the carboxyl end from the vector cTapi.289.gw (Rohila *et al.*, 2004). When both constructs were co-expressed in *N. benthamiana* cells and protein extracts incubated with a GFP nanobody fused to magnetic beads, the eluting solution included both CO and FKBP12 (Figure S2b, ELUTION FK-TAP/CO-YFP lane) none of the other controls showed a positive result (Figure S2b, ELUTION) using specific αCO and αFKBP12 (αFK) antibodies (see Experimental Procedures).

In the confocal images and co-immunoprecipitation (co-IP) experiments in *N. benthamiana*, we had observed that CO–YFP protein abundance seemed to be enhanced in the presence of TAP-tagged FKBP12, while the stability of the YFP-tagged version of CO expressed alone was drastically reduced (Figure S3b). Therefore, it was interesting to test if altering the native ratio of the proteins modified their stability – so we analyzed the presence of FKBP12 in total protein extracts from Arabidopsis Col-0, plants overexpressing *CO* (35S:*CO*) (Onouchi *et al.*, 2000) and the T-DNA null mutant co-*10* (Sail collection) (Laubinger *et al.*, 2006) employing αFK in immunoblots (Figure 1d). While the presence of FKBP12 was not altered in *co-10* mutant plants compared with the Col-0 wild type (WT) (Figure 1d), an increase in the 12 kDa immunophilin band could be detected in protein extracts from plants overexpressing *CO*. Similarly, the presence of CO in the nucleus was augmented in Arabidopsis plants overexpressing *FKBP12* (see below) when compared with WT Col-0 extracts at comparable levels to that of plants overexpressing *CO* (Figure 1e).

Altered levels of *FKBP12* expression promote variations in flowering time

Because of interaction between FKBP12 and CO, the enhanced stability of the proteins and the pivotal role of CO in the floral transition, we wondered if modifying the expression of the immunophilin would alter flowering time in Arabidopsis. To test this possibility, two different T-DNA insertion mutants (Col-0 background) in the *FKBP12* genomic region were identified – one from the Salk collection (SalK_064494) named *fk12-1* and another from the Wisconsin collection (WiscDsLox1E10) named *fk12-5*. After confirming the insertion sites of the two T-DNAs (Figure S4a, b), we obtained homozygous lines with a strong reduction in FKBP12 protein levels (Figure S4c). Both mutants showed a similar late flowering phenotype (see below) and were used for further experiments.

We then compared the expression of *FKBP12* in 24-h experiments in Col-0 and *fk12-1* (Figure 2). In LD conditions, *FKBP12* mRNA expression showed a peak 4 h after dawn (zeitgeber time 4, ZT4) and a minimum expression in the middle of the day at ZT8, slowly rising through the evening and night (Figure 2a left, grey line). In SD conditions, the pattern lacked the peak at ZT4 and showed a maximum expression at ZT12 (Figure 2a right, grey line). The expression of *FKBP12* was also followed in plants grown for 2 weeks under LDs and then transferred to either continuous light (LL) or continuous dark (DD) conditions, and mRNA accumulation was measured during the following 48 h (Figure S5). In LL conditions (Figure S5a), *FKBP12* expression continued its rhythmic tendency through two consecutive days in continuous light. When this pattern was analyzed with the Bioconductor R package RAIN ('rhythmicity analysis incorporating non-parametric methods') a significant (*P*-value = 0.05) periodic waveform was obtained, indicating the circadian character of the expression of the gene in LL conditions. However, when plants were transferred to DD, *FKBP12* expression drastically decreased, and no significant (*P*-value = 0.53) periodic pattern was observed (Figure S5b). *FKBP12* expression was significantly reduced in the mutant *fk12-1* background in LD and SD conditions, promoting the loss of circadian regulation of the gene (Figures 2a and S5c,d, black dotted lines). The reduced gene expression caused a drastic reduction in protein levels throughout the day, as shown in the immunoblots and graphics of Figure 2(b). While FKBP12 protein showed increasing accumulation during the evening in LD conditions (Figure 2b, grey line), the protein was almost completely absent in *fk12*-1 and *fk12-5* mutants (Figures 2b, black dotted line, and S4c).

To generate *FKBP12* overexpression lines, the ORF was cloned behind the 35S promoter in the pEG100 vector (Earley *et al.*, 2006) and transformed into Arabidopsis Col-0 plants by floral dipping. Selection with BASTA produced herbicide-resistant plants, from among which three T_3 independent homozygous lines were selected. *FKBP12* expression in all 35S:*FKBP12* (35S:*FK*) plants was up to seven times higher than that of WT expression in LD and SD conditions (Figure S5c,d) and this resulted in a constant and very high presence of the protein during the entire photoperiod (Figure 2b, solid black line). On the other hand, as was observed *in vitro* previously (Figure 1d), the stability and presence of FKBP12 protein increased in plants overexpressing *CO* (Figure 2c), so that the amount of immunophilin closely followed that of CO during LDs in 35S:*CO* plants, hinting again at a close association between both proteins.

In order to understand the possible effect of FKBP12 on CO function, we analyzed the 24-h expression patterns of *CO* and its primary target *FT* in *fkbp12* mutant backgrounds. We did not detect a significant modification in

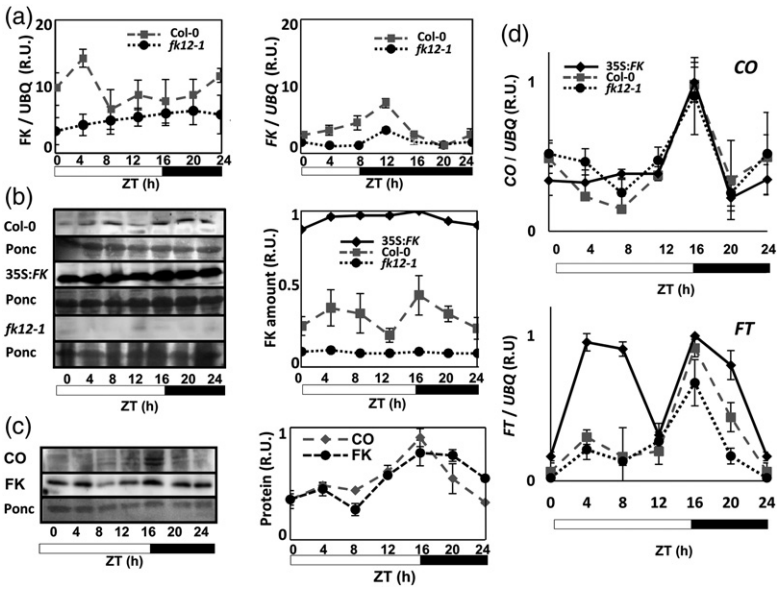

Figure 2. Molecular characterization of FKBP12 expression.
(a) Twenty-four-hour quantitative RT-PCR analysis of FKBP12 expression in Col-0 (grey) and *fk12-1* mutant (black) plants under long-day (LD; 16-h light/8-h dark) (left) and short-day (SD; 8-h light/16-h dark) (right) conditions. Ubiquitin (UBQ) was used as a control. Error bars indicate the SD from three independent experiments.
(b) Twenty-four-hour presence of FKBP12 in total protein fractions of Col-0, 35S:FK and *fk12-1* plants 15 days after germination (DAG) under LD conditions (left) and quantification of protein levels in three replicates by Western blot using αFK (right). Forty micrograms of protein was loaded per lane.
(c) Twenty-four-hour immunoblot analysis of CONSTANS (CO, above, left) and FKBP12 (FK, below, left) using αCO and αFK in total protein fractions from 35S:CO plants (15 DAG, LD). The graphic (right) represents CO and FKBP12 levels from three protein extracts compared with the control. Forty micrograms of protein was loaded per lane.
(d) Twenty-four-hour quantitative RT-PCR analysis of CO expression (above) and FT expression (below) in Col-0, *fk12-1* and 35S:FK plants (15 DAG, LD). The *UBQ* gene was used as a control. Error bars indicate SD from three independent experiments.

CO transcript levels, which maintained the same expression patterns throughout LDs in WT, *fk12-1* and overexpressing plants (Figure 2d, above). However, *FKBP12* overexpression caused a high increase in *FT* mRNA levels, particularly during the morning (ZT4–ZT8) (Figure 2d, below, solid line); as *CO* expression is not modified, this hinted at a post-translational modification of CO protein activity. On the contrary, the mutant *fk12-1* showed a slight decrease in *FT* expression, particularly during the evening when CO activates *FT* expression (Figure 2d, below, black dotted line), again revealing a possible post-translational modification of CO activity. Consistent with a role of FKBP12 in CO activity, the flowering time of *FKBP12* mutants and overexpressors were not significantly altered in SD conditions (Figure S6a), a photoperiod condition in which CO is not expressed during the day and the protein is not detectable (Suárez-López *et al.*, 2001; Valverde *et al.*, 2004). Similarly, the SD 24-h mRNA expression profiles of *CO* in WT, *fk12-1* mutant and 35S:*FK* plants (Figure S6b, left) did not show any significant change, and this was also reflected in very low expression of *FT* in the same conditions (Figure S6b, right).

To further characterize the effect of FKBP12 in CO protein activity, we isolated nuclei from Col-0, *fk12-5* and 35S:*FK* plants and detected CO and FKBP12 protein levels (Figure 3a). While the presence of FKBP12 protein in the nucleus was low in WT and *fk12-5* mutant nuclei, the amount of protein in 35S:*FK* nuclei was very high (Figure 3a). In the same blots, the upper band of CO, which represents the phosphorylated, active form (Sarid-Krebs *et al.*, 2015), was clearly visible in the 35S:*FK* plants compared with the *fk12-5* mutant and Col-0 (Figure 3a, above). When these bands were quantified in three replicates and plotted (Figure 3a, below left) a significant amount of the phosphorylated band could be detected in the 35S:*FK* plants compared with Col-0 and the *fk12-5* mutant. Furthermore, when we plotted the ratio of upper phosphorylated CO to the lower unphosphorylated form, which represents the active composition of native CO (Sarid-Krebs *et al.*, 2015), there was a significant reduction in the mutant and an increase in the 35S:*FK* plants (Figure 3a, below right). Indeed, these differences were reflected in the amount of FT protein present in total extracts of these plants in LD conditions at ZT4 (Figure 3b), with *fk12-1* and *fk12-5* (Figure S7e) mutants showing a significant decrease in FT levels and different 35S:*FK* transformants showing a significant increase compared with Col-0 (Figures 3b, right, and S4d). In these blots the presence of FKBP12 in Col-0 total extracts was always higher than in nuclear extracts, indicating a preferred non-nuclear localization as shown in the

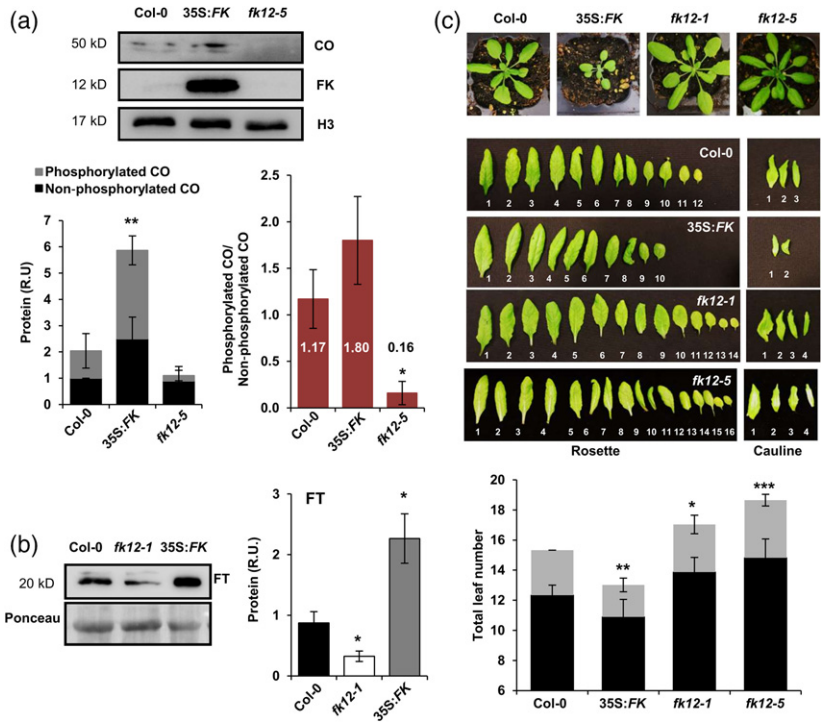

Figure 3. Flowering signals associated with FKBP12 levels.
(a) Immunoblots showing levels of CONSTANS (CO) and FKBP12 in nuclear fractions of Col-0, 35S:FK and *fk12-5* plants at 15 days after germination (DAG) (zeitgeber time 16, ZT16) under long-day (LD; 16-h light/8-h dark) conditions (above). One hundred micrograms of protein from nuclear lysates was probed with αCO, αFK and αH3. The CO signal was quantified as phosphorylated (upper) and non-phosphorylated (lower) forms compared with control, in three independent experiments and plotted (below, left). The ratio of phosphorylated (upper) and non-phosphorylated (lower) forms was quantified and compared with control in three independent experiments and plotted (below, right).
(b) Immunoblots showing FLOWERING LOCUS T (FT) in total soluble fractions of Col-0, *fk12-1* and 35S:FK plants (15 DAG, LD, ZT4) (left). Seventy micrograms of protein was loaded per lane and probed with αFT. The FT signal was quantified compared with control in three independent experiments and plotted (right).
(c) Comparison of flowering time (above) and rosette and cauline leaves (middle) in Col-0, 35S:FK, *fk12-1* and *fk12-5* plants under LD conditions. Graphic bar showing flowering time of Col-0, 35S:FK, *fk12-1* and *fk12-5* plants under LD conditions (below). Black bars, rosette leaves; grey bars, cauline leaves. Error bars indicate SD of at least 50 plants. Asterisks indicate statistically significant differences from Col-0: $*P < 0.05$; $**P < 0.01$; $***P < 0.001$.

confocal images of FK–CFP (Figure S2a), while in 35S:*FK* plants FKBP12 was very abundant in both localizations.

At a phenotypical level, we checked *FKBP12* mutants and overexpressor plants in LD conditions for a modification of flowering time in Arabidopsis (Figure 3c). Indeed, plants overexpressing *FKBP12* showed a significant small acceleration of flowering time, while *fk12*-1 and *fk12-5* mutants showed a small but significant late flowering phenotype in LD conditions (Figure 3c, middle). Wild-type plants flowered in LDs at an average of 15.3 leaves, while *fk12-1* plants flowered with 17.1 leaves, *fk12-5* with 18.6 and 35S:*FK* with 13.0 leaves, all with a high degree of significance (Figure 3c, below). Therefore, while Col-0 plants were starting to bolt 21 days after germination (DAG), the immunophilin overexpressor was already fully bolting and the mutants had not yet flowered (Figure 2c, above).

To better characterize *CO* and *FKBP12* interaction at a genetic level, we crossed plants overexpressing *CO* (35S:*CO:TAP*; Ortiz-Marchena *et al.*, 2014) and *fk12-1* plants. During the F_1 segregation we scored the flowering time of the plants in LD conditions and compared this with the flowering time of the parental plants and Col-0 (Figure S7a). As expected for a regular Mendelian distribution, flowering time of the F_1 population showed a three-modal disposition with a clear displacement of flowering time of the 35S:*CO*:*TAP* plants to the late flowering phenotype. Indeed, when we transformed 35S:*CO* constructs (Lucas-Reina *et al.*, 2015) into the *fk12-1* mutant background, selected for *CO* overexpression vector resistance (BASTA) and sowed in soil a mixture of six T_1 independent transformant seeds, a displacement of flowering time of the T_2 population plants to a late flowering phenotype was also observed (Figure S7b). This was again consistent with a delay in the early flowering phenotype of *CO* overexpression caused by the absence of *FKBP12*, which could also be observed in the floral phenotype of the homozygous plants in LD conditions (Figure S7c): 35S:*CO fk12-1* flowered with 14.7 leaves, *fk12-1* with 19.8 leaves and 35S:*CO* with 8.9 leaves. In fact, total protein extracts of 35S:*CO fk12-1* plants showed a significant increase in CO protein

when compared with the single mutant, but the distribution of the phosphorylated to unphosphorylated form was lower (Figure S7d) than in 35S:*CO* plants (compare with Figure 1e).

The CO protein is stabilized by FKBP12

The FKBP immunophilins can function as proline *cis–trans* isomerases and as molecular chaperones that help stabilize proteins and facilitate their intracellular movement (Geisler and Bailly, 2007; Gollan *et al.*, 2012). CONSTANS is strongly influenced by several different post-translational modifications, so that its final structure is likely to be important for its function and stability (Valverde *et al.*, 2004). To find out the effect of FKBP12 on the stability of CO, we again expressed both proteins in *E. coli* using the pETDuet-1 vector, but this time as a His-tagged CO (H·CO) and an S-tagged FKBP12 (S·FK). We observed that the lack of immunophilin had no effect on the amount of CO in total cell crude lysates (Figure 4a, left), but significantly reduced the amount of CO in soluble fractions (Figure 4a, right), indicating that CO solubility was enhanced by the presence of FKBP12.

In human cells, interaction of FKBP12 with TOR kinase depends on the macrolide drug rapamycin (sirolimus) that forms a strong molecular bridge between the immunophilin and the kinase, inhibiting its phosphorylating activity (Shimobayashi and Hall, 2014). Other drugs, such as FK506 (tacrolimus) can strongly bind human FKBP12 and influence the interaction with calcineurin phosphatase, inhibiting T-lymphocyte calcium-dependent signal transduction such as the transcription of *interleukin*-2 (Liu *et al.*, 1991). It has been shown that plant rapamycin does not form a molecular bridge between TOR and FKBP12 (Menand *et al.*, 2002), rendering plants immune to rapamycin, but no experiments have been performed with other drugs and targets. Both rapamycin and FK506 seemed to have no effect on single H·CO retention in a cobalt column (Figure 4b, left). When we incubated protein extracts from H·CO/S·FK-producing bacteria with rapamycin, ran the extract through the column, washed and eluted, again no difference in either FKBP12 retention or CO stability was detected in immunoblots (Figure 4b, middle, Rap). Nevertheless, when the same extracts were incubated with FK506, H·CO could not bind to the column with the same affinity (Figure 4b middle; right, FK506) and very little S·FK co-eluted with H·CO. In fact, S·FK was eluted in the washing steps (not shown). These results suggest that while rapamycin does not bind Arabidopsis FKBP12, and therefore does not affect CO interaction, this is not the case with FK506 that seems to bind FKBP12 and interfere with CO interaction, although a deeper biochemical characterization would be needed to confirm this point.

The CO protein has three distinct domains (Figure S8a), the two amino terminal b-boxes are involved in protein–protein interaction, the middle part in transcriptional activation and the C-terminal domain (CCT) in nuclei import as well as DNA and protein interactions (Wenkel *et al.*, 2006; Tiwari *et al.*, 2010). In order to identify the CO domains involved in interaction with FKBP12, we performed Y2H assays. We cloned the three parts of CO in the bait vector pJG4-5 and the complete ORF of FKBP12 in the prey vector pEG202. The resulting yeast growth and X-Gal assay (see Experimental Procedures) showed that FKBP12 interacted strongly with the CCT part of CO, while very weak interaction was observed with the amino and middle domains of the protein (Figure 4c). These results were repeated in transient bimolecular fluorescence complementation (BiFC) assays in *N. benthamiana* in which we co-transformed the N-terminal part of YFP fused to these same domains and fused C-terminal YFP with FKBP12 (Figures 4d and S9a,c–e). As expected, a strong YFP nuclear–cytosolic signal was observed under the confocal microscopy with the CCT part of CO (Figure 4d, rightmost panel) and only a weak one with the middle domain and the b-boxes (Figure 4d, left and middle panels). The finding suggested that FKBP12–CO interaction occurred mainly through the C-terminal domain, which has been proposed to interact with the E3 ligase COP1 and DNA (Jang *et al.*, 2008; Tiwari *et al.*, 2010). As interaction of CO with pseudo response regulators (PRRs) has also been proposed to involve this domain (Hayama *et al.*, 2017), this suggests that CO could bind in a supramolecular complex to DNA and FKBP12, affecting this complex formation or stabilization.

Mapping CO–FKBP12 protein interaction

FKBP12 belongs to a family of prolyl *cis–trans* isomerases involved in modifying proline topology within the polypeptide chain (Gollan *et al.*, 2012). The CO amino acid sequence shows the conservation of three valine–proline pairs (Figure S8a, red VP, above), which are particularly well conserved in a subclade of the CO phylogenetic tree (Figure S8b, C). This clade contains CO orthologs from *Chlamydomonas* (CrCO), *Physcomitrella patens* (PpCOL1–3) and Arabidopsis (AtCOL1–5) (Serrano *et al.*, 2009; Valverde, 2011) and constitute a set of CO-like proteins (COLs) whose function has been conserved throughout the phylogenetic tree of green plants (Figure S8b, red clade). Due to their high level of conservation in the evolutionary history of COL proteins, prolines in these VP pairs were good candidates to be targeted by FKBP12 activity in order to modify CO structure. Therefore, we produced a modified CO* with prolines 215, 266 and 371 substituted by alanines (Figure S8a, below, VA).

First, when we co-expressed H·CO* with S·FK using the pETDuet-1 vector in *E. coli*, the mutant protein showed a marked reduction in solubility compared with the native version (Figure 5a). The amount of CO protein in soluble extracts from bacteria producing the native H·CO protein

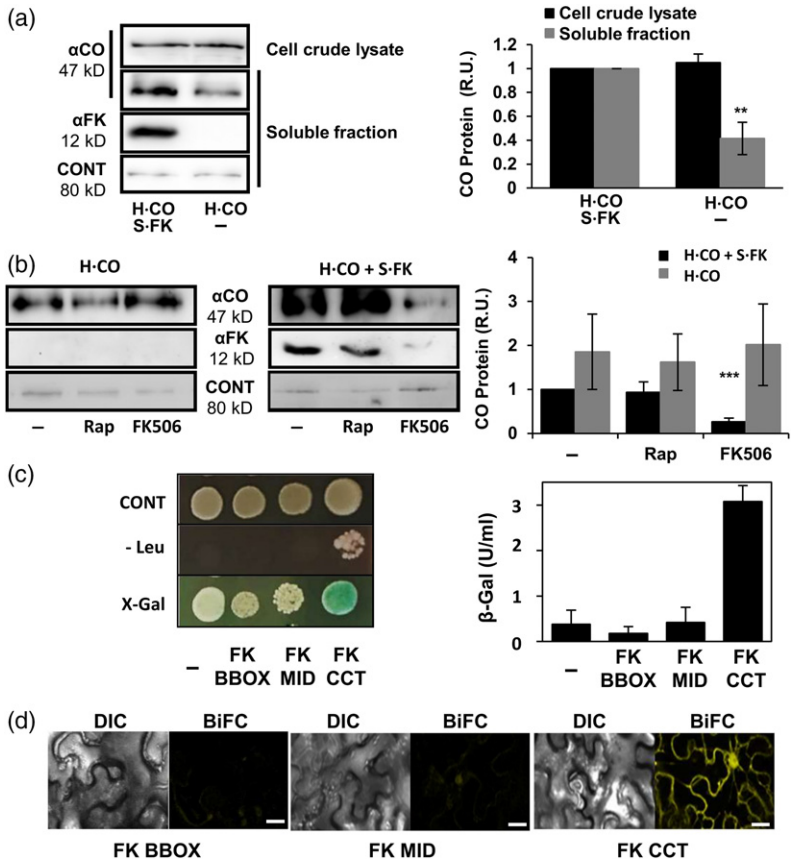

Figure 4. CONSTANS (CO) is stabilized by FKBP12.
(a) Immunoblots (left) and quantification of CO levels (right) expressed alone (H·CO) and co-expressed with FKBP12 (H·CO S·FK) in bacteria. Thirty micrograms of protein was loaded per lane and probed with αCO and αFK. Non-specific bands were used as loading controls (CONT). Right: bar graphs representing the means of CO protein amounts (± SD) in cell crude lysates (black columns) and soluble fractions (grey columns) from at least three independent experiments.
(b) Immunoblots using αCO and αFK showing column elution of H·CO (left panels) and H·CO S·FK (middle panels) extracts after rapamycin (Rap) and FK506 treatments. Non-specific bands were used as loading controls (CONT). Right: bar graph showing quantification of the amount of CO in the experiments on the left, representing the means (± SD) of at least three independent experiments.
(c) Yeast two-hybrid analysis of the interaction between FKBP12 (FK) and different domains of CO (BBOX, MIDdle and CCT). Left: interactions are shown by blue dye (X-Gal, lower panel) and growth on selective media (–Leu, middle panel). Growth on normal media is also shown (CONT, upper panel). Yeast transformed with empty plasmid pEG202:pJG4-5 (–) was used as a negative control. Pictures show 3-day-old colonies. Right: quantification of β-galactosidase (β-Gal) activity (β-Gal units × 10^4).
(d) Confocal images of bimolecular fluorescence complementation (BiFC) analysis in *Nicotiana benthamiana* epithelial cells showing protein–protein interactions between different domains of CO (BBOX, MIDdle and CCT). The white bars represent 26 μm (DIC, Differential interference contrast), Asterisks indicate statistically significant differences: $^{**}P < 0.01$; $^{***}P < 0.001$

and S·FK was significantly reduced (around 60%) in immunoblots when H·CO* was expressed together with S·FK compared with WT H·CO protein (Figure 5a, second panel). This was not due either to a reduction of CO protein in cell crude lysates (Figure 5a, first panel) or to reduced presence of FKBP12, which was found to be equivalent in both extracts (Figure 5a, third panel). Next, we performed transient BiFC assays in tobacco cells between CO*–FKBP12, and again the interaction differed from that of the WT (Figures 5b and S9a,b,g). While CO–FKBP12 interaction showed a specific nuclear localization (Figure 5b, above), the CO*–FKBP12 YFP signal was delocalized (Figure 5b, below). Nevertheless, when we tested by Y2H assay the interaction between FKBP12 and the VP-VA mutated form of the CCT domain at the three prolines (CTT*, Figure S10) there was no significant difference from the interaction with the WT domain. This could indicate either that a plant-specific post-translational modification of the CCT domain is not present in yeast (e.g. a phosphorylation event) or that although the stability of the protein and its cellular localization are compromised in the triple VA mutant this is not due to a direct lack of interaction between FKBP12 and the prolines of the VP pairs.

Interaction of FKBP12 and CO is conserved in microalgae

Chlamydomonas reinhardtii is a chlorophyte microalga used as a model photosynthetic protist; its genome is fully sequenced and annotated (Merchant *et al.*, 2007).

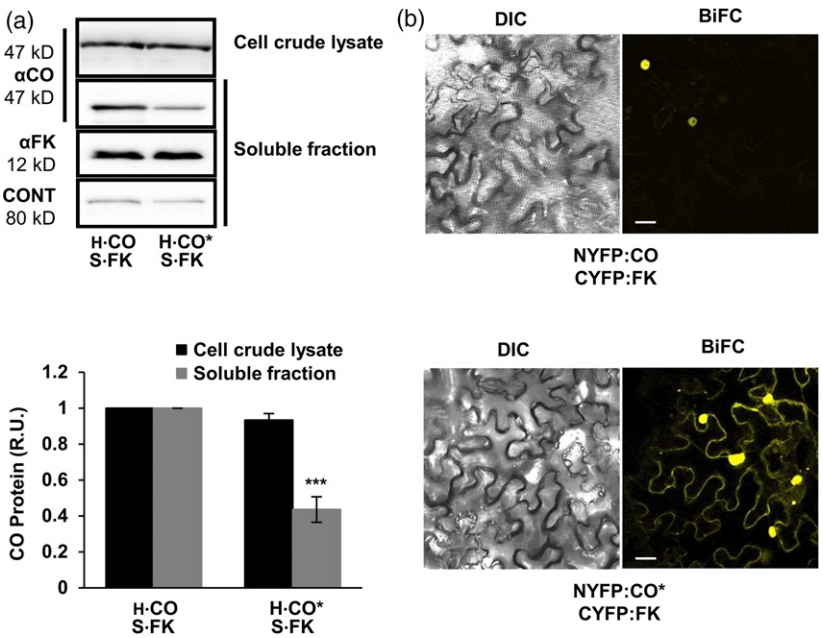

Figure 5. Interaction between FKBP12 and CONSTANS (CO) is destabilized by CO mutation in valine–proline (VP) pairs.
(a) Immunoblot analysis (above) and bar graph showing the quantification (below) of H·CO and H·CO* levels co-expressed with S-tagged FKBP12 (S·FK) in bacterial soluble fractions (black columns) and total cell crude lysates (grey columns). Thirty micrograms of protein was probed with αCO and αFK. Extracts from bacteria carrying empty plasmids were used as negative controls (−). Non-specific bands were used as loading controls (CONT). Bar graphs represent the means (± SD) of at least three independent experiments.
(b) Confocal images of bimolecular fluorescence complementation (BiFC) analysis in *Nicotiana benthamiana* epithelial cells showing protein–protein interactions between NYFP:CO and CYFP:FK (above) and NYFP:CO* and CYFP:FK (below). The white bars represent 10 μm.

Chlamydomonas has a single CO ortholog identified as CrCO, which is involved in the photoperiodic control of starch accumulation and synchronic reproduction, showing a nuclear localization (Serrano *et al.*, 2009). *Chlamydomonas* is sensitive to rapamycin, which acts as a bridge to inhibit TOR kinase through the irreversible interaction with CrFKBP12, promoting growth arrest (Crespo *et al.*, 2005). To test if the interaction we had found in Arabidopsis was conserved in algae, we first cloned *CrFKBP12* fused to *YFP* behind a constitutive promoter (p*Rbcs*/*Hsp90*:*CrFKBP12*:*YFP*) and transformed *Chlamydomonas* cells. Next, we used the nucleic acid dye (SYTO Blue 45) to report *in vivo* the presence of the nucleus (Lucas-Reina *et al.*, 2015). Observation of untransformed *Chlamydomonas* treated with SYTO blue 45 under a confocal microscope showed a distinct blue fluorescence signal in the nucleus (Figure 6a, above). When algae carrying the p*Rbcs*/*Hsp90*:*CrFKBP12*:*YFP* construct were incubated with SYTO Blue 45 and observed under a confocal microscope both yellow and blue signals coincided, reporting the nuclear presence of FKBP12 in the alga (Figure 6a, below).

Finally, to show interaction of CrCO with CrFKBP12 we performed BiFC experiments in *N. benthamiana* epidermal cells, and an intense fluorescence signal was observed at both the cytosol and the nuclear compartments (Figures 6b, left, and S9a,b,h,i). Similarly, we also tested the fluorescence complementation between Arabidopsis CO and *Chlamydomonas* CrFKBP12 (Figure 6b, middle) and, reciprocally, between *Chlamydomonas* CrCO and Arabidopsis AtFKBP12 (Figure 6b, right). Both combinations reported a strong signal, hinting at a conserved interrelation between algae and plant homologs and showing the probable conservation and importance of this interaction among photosynthetic eukaryotes.

DISCUSSION

CONSTANS activity is crucial for promoting photoperiod-dependent flowering in Arabidopsis and a significant number of plants from different taxonomic families (Yano *et al.*, 2000; Yang *et al.*, 2014; Kurokura *et al.*, 2017). *CO* is controlled at the expression level by the circadian clock through a set of clock-controlled TFs such as CYCLING DOF FACTORS (CDFs) and FLOWERING BHLHs (FBHs) that are central to its transcriptional regulation (Imaizumi *et al.*, 2005; Ito *et al.*, 2012). Besides, it has also been shown that control of its activity takes place at the post-translational level (Shim *et al.*, 2017). In this sense, the regulation through photoreceptor-dependent degradation (Valverde *et al.*, 2004), the COP1/HOS1 E3-ubiquitin ligases establishing night/day degradation by the proteasome (Jang *et al.*, 2008; Lazaro *et al.*, 2012), the building of supramolecular complexes to bind DNA (Wenkel *et al.*, 2006) and the phosphorylation of its active form (Sarid-Krebs *et al.*, 2015) seem to be essential for its mechanism of action. Here, we

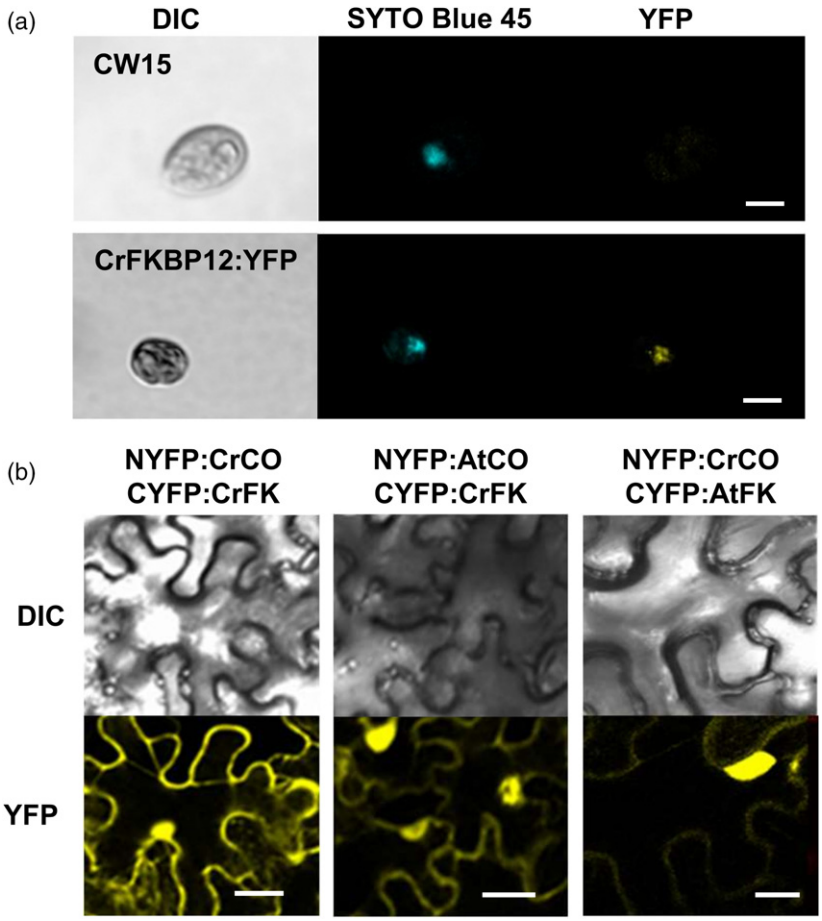

Figure 6. FKBP12 is conserved in the photosynthetic linage.
(a) Subcellular localization of *Chlamydomonas reinhardtii* FKBP12 (CrFKBP12). Confocal images of CW15 cells expressing CrFKBP12:YFP (below) and CW15 cells transformed with empty plasmid (Above) as negative controls. SYTO Blue 45 staining was used as nuclear marker. The white bars represent 10 μm.
(b) Confocal images of bimolecular fluorescence complementation (BiFC) analysis in *Nicotiana benthamiana* epithelial cells showing protein–protein interactions between NYFP:CrCO–CYFP:CrFKBP12 (left), NYFP:AtCO–CYFP:CrFKBP12 (middle) and NYFP:CrCO–CYFP:AtFKBP12 (right). The white bars represent 26 μm (left and middle) and 14 μm (right).

report a different component of post-transcriptional control of CO stability mediated by interaction with the chaperone immunophilin FKBP12. In this model (Figure 7), FKBP12 (yellow squares) would interact with CO (blue circle) stabilizing the phosphorylated form in the nucleus. Binding of FKBP12 to the CO CCT domain could prevent its degradation by COP1 and allow it to be directed to DNA to trigger the expression of *FT* (An *et al.*, 2004) to promote flowering.

Although FKBP12 has been extensively studied in yeast and animals for its capacity to interact with the key growth kinase TOR through rapamycin, this interaction does not occur in plants (Gollan *et al.*, 2012). It has been proposed that the presence of an internal disulfide bridge between two conserved Cys residues could be responsible for the lack of interaction with plant TOR (Menand *et al.*, 2002) and the induction of complex formation with new partners (Xu *et al.*, 1998). FKBP12 is also the target of the immunosuppressant drug FK506 which inhibits calcineurin and blocks the T-lymphocyte transduction pathway (Liu *et al.*, 1991). In a plant scenario, we describe here a different role for FKBP12 in which its interaction with CO would have an effect on flowering time and would be disrupted by FK506. Although it has been shown that *Vicia faba* FKBP12 cannot constitute a stable union with FK506 and calcineurin (Xu *et al.*, 1998), in our case FK506 seemed to have an effect on formation of the CO–FK506–FKBP12 ternary complex (Figure 4b). Although more rigorous tests will be needed to confirm this point, we could predict a scenario in which the addition of FKBP12 inhibitors could have a use in the agricultural industry to alter flowering time by affecting the interaction between CO and FKBP12.

Disrupting CO–FKBP12 interaction would have an effect on CO stability that can also be seen when we mutate key VP residues in the CO sequence (Figure 5a,b). Interaction with the E3 ubiquitin ligases that promote degradation of CO has been proposed to occur at the CCT domain (Lazaro *et al.*, 2015), the same domain that binds FKBP12 (Figure 4c,d). On the other hand, the positive effect of *FKBP12* overexpression on CO stability *in vivo* (Figure 1e) and on its capacity to activate *FT* expression, particularly in the morning (Figures 2d and S7e), the induction of the phosphorylated band in 35SFK plants (Figures 1e and 3a) and the reduction of this band in the single (Figure 3a) and 35S:*CO fk12-1* double mutant (Figure S7d) strongly support the idea that CO–FKBP12 interaction may be affecting the E3 ubiquitin interactions and promoting stabilization of

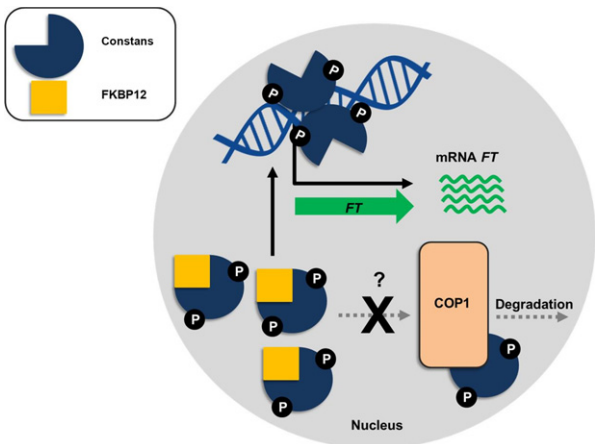

Figure 7. Molecular mechanism for interaction between CONSTANS (CO) and FKBP12.
FKBP12 interacts with CO and stabilizes the phosphorylated form in the nucleus, promoting expression of FLOWERING LOCUS T (FT) and the flowering signal (black arrows). The model suggests that FKBP12–CO interaction stabilizes the phosphorylated form by preventing CO–CONSTITUTIVE PHOTOMORPHOGENIC 1 (COP1) interaction and the following degradation of CO by the proteasome (grey arrows).

CO. However, our data cannot discard a possible effect due to its prolyl isomerase activity or to the effect of other TFs affecting flowering.

In *Picea wilsoni*, PwFKBP12 interacts with PwHAP5 (Yu *et al.*, 2011), a homolog of CO-binding partners in the HAP2/HAP3/HAP5 complex in Arabidopsis (Wenkel *et al.*, 2006). This interaction is crucial for the correct elongation of the pollen tube. Nevertheless, PwHAP5–PwFKBP12 interaction does not occur in the nucleus and must be affecting other intercellular processes. Therefore, the interaction with CO would follow a different cellular mechanism such as stability and cellular localization. In fact, the only well-characterized FKBP12 interactor in Arabidopsis is AtFIP37 (FKBP12-interacting protein 37 kDa) whose mutation causes a strong delay in endosperm development and embryo arrest (Vespa *et al.*, 2004). In the same work, Vespa and colleagues mention that the *fkbp12* mutant does not show any early developmental phenotype, but no deep description of the mutant, particularly at later stages, was given. Therefore, we provide here a more complete developmental analysis in a *fkbp12* mutant plant, and although indeed no embryo arrest or major growth failure has been detected, a closer inspection of its life cycle shows that *fk12* mutants are late flowering (Figure 3c). On the other hand, overexpression of *FKBP12* under a constitutive promoter triggered early flowering. Neither the mutant and nor the overexpression lines had any effect on accumulation of *CO* mRNA (Figure 2d), but did show an effect on the presence of CO protein in the nucleus (Figure 1e), particularly the phosphorylated form (Figure 3a), hinting to a possible role in the post-translational modification of CO activity. Correspondingly, the major target of CO, FT (Samach *et al.*, 2000), showed a clear reduced expression and abundance in *fk12* mutants, while the presence of FT was particularly high in 35S:*FK* plants (Figures 2b, 3b, S4d and S7e). In fact, in all *FKBP12ox* transformants, which are early flowering plants, *FT* expression in the morning is very high, and indeed *FT* expression in 35S:*FK* shows a bimodal expression pattern with a peak in the morning and a second peak in the evening (Figure 3d). Higher expression of *FT* in the morning has recently been reported in Arabidopsis plants growing in the wild and has been explained as being due to a greater increase in CO activity in the morning than that observed in laboratory conditions (Song *et al.*, 2018). Our results suggest likewise that *FKBP12* overexpression helps stabilize the phosphorylated and activated form of CO protein in the morning, and this is reflected in a higher production of FT and the subsequent early flowering phenotype. On the contrary, lack of FKBP12 protein will produce lower abundance of nuclear active CO protein that would promote a reduction in *FT* expression in the evening and eventually a late-flowering phenotype.

It is also remarkable that CO–FKBP12 interaction is conserved in *Chlamydomonas*, as shown by BiFC experiments with CrCO and CrFKBP12 orthologs (Figure 6b). Nevertheless, the interaction between both proteins showed a widespread nuclear–cytosolic distribution in *N. benthamiana* cells, probably reflecting differences in cellular localization between algae and plants, although new nuclear import experiments would be needed to confirm this point. The confirmation of CrCO–CrFKBP12 interaction in *Chlamydomonas* is in line with previous observations in which a conserved photoperiod response from algae to plants, sharing many common proteins, has been described (Serrano *et al.*, 2009; Lucas-Reina *et al.*, 2015). These results confirm the importance of some conserved photoperiodic regulatory tools in the evolution of photosynthetic eukaryotes (Romero and Valverde, 2009; Serrano-Bueno *et al.*, 2017).

In conclusion, as depicted in the model of Figure 7, photoperiodic flowering control mediated by CO is modulated at the post-transcriptional level by the interaction with the immunophilin FKBP12, facilitating the nuclear stability of the active form and *FT* transcription. Although we cannot discard other effects associated with FKBP12 derived from its prolyl isomerase activity or to the effect compared with other TFs involved in flowering time, CO–FKBP12 interaction seems highly conserved in the green plant lineage, and has a measurable effect on flowering time in plants, unveiling a strong evolutionary importance.

EXPERIMENTAL PROCEDURES

Plant material and growth conditions

Arabidopsis thaliana L. Heynh. (thale cress) WT were of the Columbia (Col-0) ecotype. The T-DNA insertion mutant *fk12-1*

(SALK_064494.47.85.x) was obtained from the SALK collection, while the *fk12-5* mutant (WiscDsLox1E10) was obtained from the Wisconsin collection. For 35S:*FK* lines, full-length cDNA (RIKEN, https://www.riken.jp/en/) was cloned into a pEarleyGate 100 vector (Earley *et al.*, 2006) behind the CaMV 35S promoter or in the cTapi.289.gw (Rohila *et al.*, 2004) to obtain the FK-TAP version. For each recombinant plant at least 10 individuals were initially isolated, with three plants, showing a homogeneous phenotype, finally being selected for the analysis. Plants were grown in controlled cabinets on peat-based compost (for flowering time determination, FRET and BiFC assays) or on MS plates (for quantitative RT-PCR assays and protein determinations). Seeds were previously incubated for 4 days at 4°C in the dark before sowing under LD cycles with temperatures ranging from 22°C (day) to 18°C (night).

Pull-down assays in bacteria

Full-length *CO* and *FKBP12* coding sequences (CDSs) were cloned into the pETDuet-1 vector (Novagen, https://www.merckgroup.com) and introduced into *E. coli* BL21 cells. S·CO/ H·CO and H·FK/ S·FK versions were induced by 4 h incubation with 1 mM IPTG (Applichem, https://www.applichem.com) at 30°C. S·CO was immobilized on protein A magnetic beads (Diagenode, https://www.diagenode.com) previously charged with S·tag antibody (Novagen). For pull-down assays, H·FK was incubated with the immobilized S·CO for 2 h at 4°C. Proteins were detected by immunoblot using αCO (raised in rabbit against the CO middle domain as described in Valverde *et al.*, 2004), αFKBP12 (this work, see below), αFT (Agrisera, https://www.agrisera.com/) and αHis antibodies (Qiagen, https://www.qiagen.com/). Loading controls for nuclei extracts were histone 3 antibody (Abcam, https://www.abcam.com/) and for cytosol extracts an antibody against recombinant non-phosphorylating GAPDH (GAPN) as described in Valverde *et al.* (1999).

Yeast-based protein interaction analysis

The SUS was as in Pusch *et al.* (2012), using a cDNA library from F. Santos, I. Ottenschläger and K. Palme (Max Planck Institute for Plant Breeding. Research, Cologne, Germany). CONSTANS was cloned in the bait vector pMET-Cub-R-URA and cDNA in the prey vector pCU-Nub and transformed into the JD53 yeast strain. Cells were plated onto minimal SD medium plates +/− Ura supplemented with 25 μM Met and 100 μM copper sulfate for growth control, or on SD plus 1 mg/ml FOA, 25 μM Met and 100 μM copper sulfate for clone rescue. Cells were grown at 30°C for 3 days, surviving clones identified, DNA rescued by plasmid extraction and tested by PCR. For Y2H assays, CO domains CCT, CCT*, middle and bbox domains were cloned into the bait vector pJG4-5, while the full-length *FKBP12* CDS was cloned into the prey vector pEG202. The primers used to generate Y2H clones are listed in Table S1. EGY48 (MATα *trp1 ura3 his3 LEU2::pLex Aop6-LEU2*) was used as the host strain for Y2H experiments (Gyuris *et al.*, 1993). Positive interactions were detected by a blue color on Ura–His–Trp X-gal plates and survival on GAL–Ura–Trp–His–Leu selective plates. For quantitative assays, the transformants were grown at 30°C to 0.5–0.8 OD 600 nm. The β-gal activity (U ml^{-1}) in Figure 4(c) was measured at OD 420 nm using *o*-nitrophenyl β-D-galactopyranoside (Sigma, https://www.sigmaaldrich.com/).

Protein analysis

Arabidopsis proteins were isolated from 14-DAG seedlings grown in MS plates employing the TRIzol (Invitrogen, https://www.thermofisher.com) protocol as described by the manufacturer. Nuclear-enriched fractions were obtained from Col-0, 35S:*CO*, 35S:*FK*, *fk12-1*, *fk12-5*, 35S:*CO fk12-1* and 35S:*CO*:*TAP* tag (Ortiz-Marchena *et al.* 2014) seedlings grown on MS plates for 2 weeks as described (Lazaro *et al.*, 2012). *FKBP12*, *CO* and *CO** expressed in *E. coli* BL21 cells were induced as above. Cells were disrupted using glass beads (0.5 mM) in an extraction buffer containing 0.33 mM sorbitol, 25 mM 2-amino-2-(hydroxymethyl)-1,3-propanediol (TRIS)-HCl (pH 7.5), 2 mM EDTA, 2 mM DTT, 1 mM phenylmethylsulfonyl fluoride, 1 mM benzamidine and 1 mM ϵ-aminocaproic acid and soluble fractions isolated by low-speed (5 min, 500 ***g***) followed by high-speed (15 min, 20,000 ***g***) centrifugation. The amount of protein was determined by the Bradford assay (Bio-Rad, https://www.bio-rad.com/) according to the manufacturer's instructions with ovalbumin as a standard. Proteins were separated by SDS-PAGE using standard procedures, transferred to nitrocellulose or polyvinylidene difluoride filters and probed with αCO, αFT or αFK. FKBP12 antibodies were raised in rabbit against the synthesized (Sigma) specific Arabidopsis FKBP12 peptide (NH_3-MGEVIKGWDEGVAQMC-COOH) and further purified through column-bound FKBP12-Histag. αH3 (Abcam) was used as the nuclear protein marker. Blots were developed with a chemiluminescent substrate according to the manufacturer's instructions (Immobilon Western Chemiluminescent HRP Substrate; Millipore, https://www.merckmillipore.com/).

Co-immunoprecipitation experiments were performed by transient assays in *N. benthamiana* cells as described in Lazaro *et al.* (2015). In brief, *A. tumefaciens* GV3101 (pMP90) transformed with 35S:*FKBP12*:*TAP* (FK-TAP), 35S:*CO*:*YFP* (CO-YFP) or a combination of both were infiltrated in young leaves of *N. benthamiana* as described below. After 3 days, 1 g of infected tissue or negative control (only p19) was ground with a mortar and pestle in the presence of liquid nitrogen and resuspended in 2 ml co-IP buffer (Lazaro *et al.*, 2015). After centrifugation for 10 min at 2350 ***g*** in a microfuge at 4°C, 0.5 ml of supernatants was incubated with 25 μl of washed GFP-Trap®_MA nanobody beads (Chromotek, https://www.chromotek.com/) and stirred for 2 h at 4°C in a rotor incubator. After three washes in co-IP buffer, samples were eluted by adding 5× SDS-PAGE loading buffer and incubating at 95°C for 5 min.

Microscopy

For the BiFC experiments, *FKBP12*, different domains of *CO* and their *Chlamydomonas* orthologs were cloned in pYFN43 and pYFC43 vectors (Ferrando *et al.*, 2001) to produce N-terminal fusions of the carboxyl (pYFC43) and amino (pYFN43) parts of YFP. These constructs were introduced into *A. tumefaciens* strain C58 and infiltrated in *N. benthamiana* leaves together with p19 protein (Voinnet *et al.*, 2003). The BiFC protocol was followed as previously described (Lucas-Reina *et al.*, 2015). Amino and carboxyl domains of AKINβ and AKIN10 sucrose-non-fermenting (Snf1)-related kinases (SnRK) were used as positive controls (Ferrando *et al.*, 2001). Co-agroinfiltrations with empty vectors were used as negative controls. The BiFC was visualized under a Leica TCS SP2 confocal microscope (https://www.leica-microsystems.com/) set at 550 nm and analyzed with Leica LCSLite software. For the FRET experiments, CO-YFP and FK-CFP constructs were introduced into *N. benthamiana* leaves by agroinfiltration. Two to three days after transfection, epidermal cells were visualized using a Leica TCS SP2/DMRE microscope equipped with a 63× objective lens. Excitation of CFP was with a 458 nm laser and that of YFP with a 514 nm laser. Band-pass filters were adjusted to 465–479 nm and 520–545 nm in the CFP and YFP detection channels, respectively. The acceptor photobleaching technique was used to measure FRET, thus regions of interest (ROIs) were bleached using the argon-ion laser at high intensity to remove fluorescence of the acceptor. Ten

cell nuclei were imaged to quantify the change in donor fluorescence and FRET efficiency was measured according to the formula (pre-bleaching – post-bleaching)/(pre-bleaching). An electroporation protocol was used for *C. reinhardtii* nuclear transformation (Lucas-Reina *et al.*, 2015). CW15 and several *CrFKBP12*:*YFP* transgenic lines were observed under the confocal microscope together with SYTOBlue45 Fluorescent Nucleic Acid Stain (Molecular Probes, https://www.thermofisher.com/). Algae were grown under SD conditions in Sueoka medium supplemented with 10 mM NO_3 until lag phase (3–4 μg ml^{-1} chlorophyll). One milliliter of this was collected by centrifugation (4 min, 5500 ***g***) and suspended in 1 ml TRIS-buffered saline buffer. One microliter of SYTOBlue45 and 1 and 5 μl of 10% (v/v) Triton X-100, for CW15 cells and transgenic lines respectively, was added. After incubation for 10 min, cells were centrifuged and suspended in 100 μl of the same buffer. Finally, 3 μl of cells were mixed with 10 μl of 1.2% (w/v) low-point fusion agarose at 30°C. The wavelengths used were 514 nm for YFP and 458 nm for SYTOBlue45.

RNA extraction and quantitative RT-PCR

One microgram of TRIzol-isolated RNA was used to synthesize cDNA with the Quantitec Reverse Kit (Qiagen) following the manufacturer's instructions and diluted to a final concentration of 10 ng μl^{-1}. Primers for *CO*, *FT* and *UBQ10* amplification (Ortiz-Marchena *et al.*, 2014) were used in an iQTM5 multicolor real-time PCR detection system (Bio-Rad) in a 10-μl reaction: 0.2 μM primers, 10 ng cDNA, 5 μl SensiFAST TM from a SYBR Fluorescein kit (Bioline, https://www.bioline.com/). The initial concentration of candidate and reference genes was calculated by means of LingRegPCR software version 11.0 (Ruijter *et al.*, 2009). Normalized data were calculated by dividing the average of at least three replicates of each sample from the candidate and reference genes.

Analysis of flowering time

Flowering time was analyzed in controlled-environment cabinets by scoring the number of rosette (excluding cotyledons) and cauline leaves. Data are expressed as the mean of at least 20 individuals ± SE.

Site-directed mutagenesis

Site-directed mutagenesis was performed to replace the conserved VP pairs of CO to VA pairs according to the manufacturer's instructions (Muta-direct™ Site-Directed Mutagenesis, iNtRON Biotechnology, https://intronbio.com:6001). All constructs were verified by DNA sequencing. The primers used are listed in Table S1.

Statistical analysis

The statistical data are marked with asterisks and are means ± SE. of at least three biological experiments. The statistical significance between means of the different samples was calculated using a two-tailed Student's *t*-test. Differences observed were considered statistically significant at $P < 0.05$ (*), $P < 0.01$ (**) and $P < 0.001$ (***).

ACKNOWLEDGEMENTS

Funding from projects BIO2014-52425-P, BIO2017-83629-R (Spanish Ministry of Science) and P08-AGR-03582, BIO-281 (Junta de Andalucia) supported by FEDER funding is acknowledged. GS-B received financial support from the European Union (EU) project H2020-MSCA-IF-2018, GA838317. FES received a Spanish Ministry of External Affairs (AECID) fellowship and EIL-R a CSIC-JAE fellowship, partly supported by structural funding from the EU (SEF). The IBVF microscopy services (Alicia Orea) and University of Seville microscopy and glasshouse services (General Research Services, CITIUS) are also acknowledged. All authors declare that there is no conflict of interest in the publication of this article.

AUTHOR CONTRIBUTION

GS-B and FES produced most of the results data, wrote the text and made the figures. PdlR produced most of the QPCR, FRET, statistics and bioinformatics data. EIL-R produced the mutagenesis and bacterial biochemistry experiments. MIO-M produced the flowering time data and mutant analysis. JMR and FV procured funding, designed and reviewed experimental procedures, wrote the text and corrected the different versions of the manuscript.

DATA STATEMENT

All materials, figures and supporting data are available upon request from the corresponding author at federico.valverde@ibvf.csic.es.

CONFLICT OF INTEREST

The authors declare that there is no conflict of interest.

SUPPORTING INFORMATION

Additional Supporting Information may be found in the online version of this article.

Figure S1. Classification of CONSTANS interactors.

Figure S2. Subcellular localization of CONSTANS and FKBP12.

Figure S3. CONSTANS–FKBP12 interaction *in vivo*.

Figure S4. Characterization of *fkbp12* mutants.

Figure S5. Analysis of *FKBP12* circadian expression.

Figure S6. Flowering time, *CO* and *FT* expression in short-day plants.

Figure S7. Characterization of the genetic interaction between *CO* and *FKBP12*.

Figure S8. Conserved valine–proline residues and phylogenetic tree of COL proteins.

Figure S9. Bimolecular fluorescence complementation controls.

Figure S10. Interaction between CO* and FKBP12.

Table S1. List of primers used in this work.

REFERENCES

An, H., Roussot, C., Suárez-López, P. *et al.* (2004) CONSTANS acts in the phloem to regulate a systemic signal that induces photoperiodic flowering of Arabidopsis. *Development*, **131**, 3615–3626.

Andrés, F. and Coupland, G. (2012) The genetic basis of flowering responses to seasonal cues. *Nat. Rev. Genet.* **13**, 627–639.

Austen, E.J., Rowe, L., Stinchcombe, J.R. and Forrest, J.R.K. (2017) Explaining the apparent paradox of persistent selection for early flowering. *New Phyt.* **215**, 929–934.

Ben-Naim, O., Eshed, R., Parnis, A., Teper-Bamnolker, P., Shalit, A., Coupland, G., Samach, A. and Lifschitz, E. (2006) The CCAAT binding factor can mediate interactions between CONSTANS-like proteins and DNA. *Plant J.* **46**, 462–476.

Blümel, M., Dally, N. and Jung, C. (2015) Flowering time regulation in crops – what did we learn from Arabidopsis? *Cur. Opin. Biotech.* **32**, 121–129.

Crespo, J.L., Díaz-Troya, S. and Florencio, F.J. (2005) Inhibition of target of rapamycin signalling by rapamicin ib the unicellular green alga *Chlamydomonas reinhardtii*. *Plant Phys.* **139**, 1736–1749.

Cyert, M.S. (2001) Regulation of nuclear localization during Signaling. *J. Biol. Chem.* **276**, 20805–20808.

Dünnwald, M., Varshavsky, A. and Johnsson, N. (1999) Detection of transient in vivo interactions between substrate and transporter during protein translocation into the endoplasmic reticulum. *Mol. Biol. Cell*, **10**, 329–344.

Earley, K.W., Haag, J.R., Pontes, O., Opper, K., Juehne, T., Song, K. and Pikaard, C.S. (2006) Gateway-compatible vectors for plant functional genomics and proteomics. *Plant J.* **45**, 616–629.

Faure, J.D., Gingerich, D. and Howell, S.H. (1998) An Arabidopsis immunophilin, AtFKBP12, binds to AtFIP37 (FKBP interacting protein) in an interaction that is disrupted by FK506. *Plant J.* **15**, 783–789.

Ferrando, A., Koncz-Kalman, Z., Farras, R., Tiburcio, A., Schell, J. and Koncz, C. (2001) Detection of in vivo protein interactions between Snf1-related kinase subunits with intron-tagged epitope-labelling in plants cells. *Nucleic Acids Res.* **29**, 3685–3693.

Geisler, M. and Bailly, A. (2007) Tête-à-tête: the function of FKBPs in plant development. *Trends Plant Sci.* **12**, 465–473.

Gnesutta, N., Kumimoto, R.W., Swain, S., Chiara, M., Siriwardana, C., Horner, D.S., Holt, B.F. III and Mantovani, R. (2017) CONSTANS Imparts DNA Sequence Specificity to the Histone Fold NF-YB/NF-YC Dimer. *Plant Cell*, **29**, 1516–1532.

Gollan, P.J., Bhave, M. and Aro, E.-M. (2012) The FKBP families of higher plants: exploring the structures and functions of protein interaction specialists. *FEBS Let.* **586**, 3539–3547.

Guo, X., Yu, C., Luo, L., Wan, H., Zhen, N., Xu, T., Tan, J., Pan, H. and Zhang, Q. (2017) Transcriptome of the floral transition in *Rosa chinensis* 'Old Blush'. *BMC Genom.* **18**, 199.

Gyuris, J., Golemis, E., Chertkov, H. and Brent, R. (1993) Cdi1, a human G1 and S phase protein phosphatase that associates with Cdk2. *Cell*, **75**, 791–803.

Hayama, R., Sarid-Krebs, L., Richter, R., Fernández, V., Jang, S. and Coupland, G. (2017) PSEUDO RESPONSE REGULATORs stabilize CONSTANS protein to promote flowering in response to day length. *EMBO J.* **36**, 904–918.

Igarashi, D., Ishida, S., Fukazawa, J. and Takahashi, Y. (2001) 14-3-3 Proteins Regulate Intracellular Localization of the bZIP Transcriptional Activator RSG. *Plant Cell*, **13**, 2483–2498.

Imaizumi, T., Schultz, T.F., Harmon, F.G., Ho, L.A. and Kay, S.A. (2005) FKF1 F-box protein mediates cyclic degradation of a repressor of CONSTANS in Arabidopsis. *Science*, **309**, 293–297.

Ito, S., Song, Y.H., Josephson-Day, A.R., Miller, R.J., Breton, G., Olmstead, R.G. and Imaizumi, T. (2012) FLOWERING BHLH transcriptional activators control expression of the photoperiodic flowering regulator CONSTANS in Arabidopsis. *Proc. Natl. Acad. Sci. USA*, **109**, 3582–3587.

Jackson, S.D. (2009) Plant responses to photoperiod. *New Phytol.* **181**, 517–531.

Jang, S., Marchal, V., Panigrahi, K.C.S., Wenkel, S., Soppe, W., Deng, X.W., Valverde, F. and Coupland, G. (2008) Arabidopsis COP1 shapes the temporal pattern of CO accumulation conferring a photoperiodic flowering response. *EMBO J.* **27**, 1277–1288.

Johnsson, N. and Varshavsky, A. (1994) Split ubiquitin as a sensor of protein interactions in vivo. *Proc. Natl. Acad. Sci. USA*, **91**, 10340–10344.

Kang, C.B., Hong, Y., Dhe-Paganon, S. and Yoon, H.-S. (2008) FKBP family proteins: immunophilins with versatile biological functions. *Neurosignals*, **16**, 318–325.

Kim, J.E. and Chen, J. (2002) Cytoplasmic–nuclear shuttling of FKBP12-rapamycin-associated protein is involved in rapamycin-sensitive signaling and translation initiation. *Proc. Natl. Acad. Sci. USA*, **97**, 14340–14345.

Kurokura, T., Samad, S., Koskela, E., Mouhu, K. and Hytönen, T. (2017) *Fragaria vesca* CONSTANS controls photoperiodic flowering and vegetative development. *J. Exp. Bot.* **68**, 4839–4850.

Laubinger, S., Marchal, V., Gentilhomme, J., Wenkel, S., Adrian, J., Jang, S., Kulajta, C., Braun, H., Coupland, G. and Hoecker, U. (2006) Arabidopsis SPA proteins regulate photoperiodic flowering and interact with the floral inducer CONSTANS to regulate its stability. *Development*, **133**, 4608–4608.

Lazaro, A., Valverde, F., Piñeiro, M. and Jarillo, J.A. (2012) The E3 ubiquitin ligase HOS1 participates in the control of photoperiodic flowering in Arabidopsis negatively regulating CONSTANS abundance. *Plant Cell*, **24**, 982–999.

Lazaro, A., Mouriz, A., Piñeiro, M. and Jarillo, J.A. (2015) Red light-mediated degradation of CONSTANS by the E3 ubiquitin ligase HOS1 regulates photoperiodic flowering in Arabidopsis. *Plant Cell*, **27**, 2437–2454.

Levin, D. (2009) Flowering-time plasticity facilitates niche shifts in adjacent populations. *New Phytol.* **183**, 661–666.

Liu, J., Farmer, J., Lane, W., Friedman, J., Weissman, I. and Schreiber, S. (1991) Calcineurin is a common target of cyclophilin-cyclosporin A and FKBP-FK506 complexes. *Cell*, **66**, 807–815.

Loewith, R., Jacinto, E., Wullschleger, S., Lorberg, A., Crespo, J.L., Bonenfant, D., Oppliger, W., Jenoe, P. and Hall, M.N. (2002) Two TOR complexes, only one of which is rapamycin sensitive, have distinct roles in cell growth control. *Mol. Cell*, **10**, 457–468.

Lucas-Reina, E., Romero-Campero, F.J., Romero, J.M. and Valverde, F. (2015) An Evolutionarily Conserved DOF-CONSTANS Module Controls Plant Photoperiodic Signalling. *Plant Physiol.* **168**, 561–574.

Mathieu, J., Warthmann, N., Küttner, F. and Schmid, M. (2007) Export of FT Protein from Phloem Companion Cells Is Sufficient for Floral Induction in *Arabidopsis*. *Cur. Biol.* **17**, 1055–1060.

Mattioli, R., Falascb, G., Sabatini, S., Altamura, M.M., Costantino, P. and Trovato, M. (2009) The proline biosynthetic genes *P5CS1* and *P5CS2* play overlapping roles in *Arabidopsis* flower transition but not in embryo development. *Physiol. Plant.* **137**, 72–85.

Menand, B., Desnos, T., Nussaume, L., Berger, F., Bouchez, D., Meyer, C. and Robaglia, C. (2002) Expression and disruption of the Arabidopsis TOR (target of rapamycin) gene. *Proc. Natl. Acad. Sci. USA*, **99**, 6422–6427.

Merchant, S.S., Prochnik, S.E., Vallon, O. *et al.* (2007) The Chlamydomonas genome reveals the evolution of key animal and plant functions. *Science*, **318**, 245–250.

Onouchi, H., Igeño, M.I., Perilleux, C., Graves, K. and Coupland, G. (2000) Mutagenesis of plants overexpressing CONSTANS demonstrates novel interactions among *Arabidopsis* flowering-time genes. *Plant Cell*, **12**, 885–900.

Ortiz-Marchena, M.I., Albi, T., Lucas-Reina, E., Said, F.E., Romero-Campero, F.J., Cano, B., Ruiz, M.T., Romero, J.M. and Valverde, F. (2014) Photoperiodic control of carbon distribution during the floral transition in Arabidopsis. *Plant Cell*, **26**, 565–584.

Ortiz-Marchena, M.I., Romero, J.M. and Valverde, F. (2015) Photoperiodic control of sugar release during the floral transition: what is the role of sugars in the florigenic signal? *Plant Signal. Behav.* **5**, e1017168.

Pajoro, A., Biewers, S., Dougali, E. *et al.* (2014) The (r)evolution of gene regulatory networks controlling Arabidopsis plant reproduction: a two-decade history. *J. Exp. Bot.* **65**, 4731–4745.

Posé, D., Verhage, L., Ott, F., Yant, L., Mathieu, J., Angenent, G.C., Immink, R.G. and Schmid, M. (2013) Temperature-dependent regulation of flowering by antagonistic FLM variants. *Nature*, **503**, 414–417.

Pusch, S., Harashima, H. and Schnittger, A. (2012) Identification of kinase substrates by bimolecular complementation assays. *Plant J.* **70**, 348–356.

Rohila, J.S., Chen, M., Cerny, R. and Fromm, M.E. (2004) Improved tandem affinity purification tag and methods for isolation of protein heterocomplexes from plants. *Plant J.* **38**, 172–181.

Romero, J.M. and Valverde, F. (2009) Evolutionarily conserved photoperiod mechanisms in plants. When did plant photoperiodic signalling appear? *Plant Sig. Behav.* **4**, 642–644.

Ruijter, J.M., Ramakers, C., Hoogaars, W.M., Karlen, Y., Bakker, O., van den Hoff, M.J. and Moorman, A.F.M. (2009) Amplification efficiency: Linking baseline and bias in the analysis of quantitative PCR data. *Nucleic Acids Res.* **37**, e45.

Samach, A., Onouchi, H., Gold, S.E., Ditta, G.S., Schwarz-Sommer, Z., Yanofsky, M.F. and Coupland, G. (2000) Distinct roles of CONSTANS target genes in reproductive development of Arabidopsis. *Science*, **288**, 1613–1616.

Sarid-Krebs, L., Panigrahi, K.C.S., Fornara, F., Takahashi, Y., Hayama, R., Jang, S., Tilmes, V., Valverde, F. and Coupland, G. (2015) Phosphorylation of CONSTANS and its COP1-dependent degradation during photoperiodic flowering of Arabidopsis. *Plant J.* **84**, 451–463.

Serrano, G., Herrera-Palau, R., Romero, J.M., Serrano, A., Coupland, G. and Valverde, F. (2009) Chlamydomonas CONSTANS and the evolution of plant photoperiodic signaling. *Curr. Biol.* **19**, 359–368.

Serrano-Bueno, G., Romero-Campero, F.J., Lucas-Reina, E., Romero, J.M. and Valverde, F. (2017) Evolution of photoperiod sensing in plants and algae. *Curr. Opin. Plant Biol.* **37**, 10–17.

Shim, J.S., Kubota, A. and Imaizumi, T. (2017) Circadian clock and photoperiodic flowering in Arabidopsis: CONSTANS Is a hub for signal integration. *Plant Phys.* **173**, 5–15.

Shimobayashi, M. and Hall, M.N. (2014) Making new contacts: the mTOR network in metabolism and signalling crosstalk. *Nat. Rev. Mol. Cell Biol.* **15**, 155–162.

Song, J., Angel, A., Howard, M. and Dean, C. (2012) Vernalization - a cold-induced epigenetic switch. *J. Cell Sci.* **125**, 3723–3731.

Song, Y.H., Kubota, A., Covington, M.F. *et al.* (2018) Molecular basis of flowering under natural long-day conditions in *Arabidopsis*. *Nat. plants* **4**, 824–835.

Suárez-López, P., Wheatly, K., Robson, F., Onouchi, H., Valverde, F. and Coupland, G. (2001) CONSTANS mediates between the circadian clock and the control of flowering in Arabidopsis. *Nature*, **410**, 4116–4120.

Swiezewski, S., Liu, F., Magusin, A. and Dean, C. (2009) Cold-induced silencing by long antisense transcripts of an Arabidopsis Polycomb target. *Nature*, **462**, 799–802.

Tiwari, S.B., Shen, Y., Chang, H.C. *et al.* (2010) The flowering time regulator CONSTANS is recruited to the FLOWERING LOCUS T promoter via a unique cis-element. *New Phytol.* **187**, 57–66.

Valverde, F. (2011) CONSTANS and the evolutionary origin of photoperiodic timing of flowering. *J. Exp. Bot.* **62**, 2453–2463.

Valverde, F., Losada, M. and Serrano, A. (1999) Engineering a central metabolic pathway: glycolysis with no net phosphorylation in an *Escherichia coli gap* mutant complemented with a plant *GapN* gene. *FEBS Lett*, **449**, 153–158.

Valverde, F., Mouradov, A., Soppe, W., Ravenscroft, D., Samach, A. and Coupland, G. (2004) Photoreceptor regulation of CONSTANS protein in photoperiodic flowering. *Science*, **303**, 1003–1006.

Vespa, L., Vachon, G., Berger, F., Perazza, D., Faure, J.-D. and Herzog, M. (2004) The immunophilin-interacting protein AtFIP37 from Arabidopsis is essential for plant development and is involved in trichome endoreduplication. *Plant Phys.* **134**, 1283–1292.

Voinnet, O., Rivas, S., Mestre, P. and Baulcombe, D. (2003) An enhanced transient expression system in plants based on suppression of gene silencing by the p19 protein of tomato bushy stunt virus. *Plant J.* **33**, 949–956.

Wenkel, S., Turck, F., Singer, K., Gissot, L., Le Gourrierec, J., Samach, A. and Coupland, G. (2006) CONSTANS and the CCAAT box binding complex share a functionally important domain and interact to regulate flowering of Arabidopsis. *Plant Cell*, **18**, 2971–2984.

Wilson, R.S., Swatek, K.N. and Thelen, J.J. (2016) Regulation of the regulators: post-translational modifications, subcellular, and spatiotemporal distribution of plant 14-3-3 proteins. *Front. Plant Sci.* **7**, 611.

Xiong, Y. and Sheen, J. (2012) Rapamycin and glucose-target of rapamycin (TOR) protein signaling in plants. *J. Biol. Chem.* **287**, 2836–2842.

Xu, Q., Liang, S., Kudla, J. and Luan, S.W. (1998) Molecular characterization of a plant FKBP12 that does not mediate action of FK506 and rapamycin. *Plant J.* **15**, 511–519.

Yang, S., Weers, B.D., Morishige, D.T. and Mullet, J.E. (2014) CONSTANS is a photoperiod regulated activator of flowering in sorghum. *BMC Plant Biol.* **14**, 148.

Yano, M., Katayose, Y., Ashikari, M. *et al.* (2000) Hd1, a major photoperiod sensitivity quantitative trait locus in rice, is closely related to the Arabidopsis flowering time gene CONSTANS. *Plant Cell*, **12**, 2473–2484.

Yu, Y., Li, Y., Huang, G., Meng, Z., Zhang, D., Wei, J., Yan, K., Zheng, C. and Zhang, L. (2011) PwHAP5, a CCAAT-binding transcription factor, interacts with PwFKBP12 and plays a role in pollen tube growth orientation in *Picea wilsonii*. *J. Exp. Bot.* **62**, 4805–4817.